Inverse Scattering of an Embedded Inhomogeneous Dielectric Cylinders Coated on a Conductor

Chun Jen Lin, Chung-Hsin Huang and Chien-Ching Chiu

Abstract— In this paper, the inverse problem of an embedded inhomogeneous dielectric cylinders coated on a conductor by TM wave illumination is investigated. Inhomogeneous dielectric cylinders coated on a conductor embedded in a slab scatters a group of unrelated incident waves from outside. The scattered field is recorded outside the slab. By proper arrangement of the various unrelated incident field, the difficulties of ill-posedness and nonlinearity are circumvented, and the permittivity distribution can be reconstructed through simple matrix operations. The algorithm is based on the moment method and the unrelated illumination method. Numerical results are given to demonstrate the capability of the inverse algorithm. They also show that the permittivity distribution of the cylinders can be successfully reconstructed even when the permittivity is fairly large. Good reconstructed is obtained even in the presence of additive Gaussian noise in measured data. In addition, the effect of noise on the reconstruction result is also investigated.

Index Terms—Inverse scattering, Inhomogeneous Cylinders, Slab Medium, Unrelated Illumination Method.

I. INTRODUCTION

In the past years, electromagnetic inverse scattering problems of underground objects have been a growing importance in many different fields of applied science. In recent years, the electromagnetic imaging of objects buried in a slab medium has attracted considerable attention in with a large potential impact on geosciences and remote sensing and pipelines applications. However, the solutions are considerably more difficult than those involving objects in a free space and half space. This is due to the interaction between the interface of the three layers and the object, which leads to the complicated Green's function for this three layer problem. In the past, most of the research in the aspect emphasize on reconstruction of the second layer profile in the three layer structures [1]-[5]. However, only a few papers deal with the reconstruction of buried conducting objects in the three layer structures [6], [7]. To the best of our knowledge, there is still no investigation on the electromagnetic imaging of inhomogeneous dielectric

cylinders buried in a slab medium by unrelated illumination method.

In this paper, the inverse problem of an embedded inhomogeneous dielectric cylinders coated on a conductor by TM wave illumination is investigated. The algorithm is based on the method of moment [8] and the unrelated illumination method [9]. In Section 2, the theoretical formulation for electromagnetic imaging is presented. Numerical results for buried dielectric objects are given in Section 3. Finally some conclusions are drawn in Section 4.

II. THEORETICAL FORMULATION

Let us consider dielectric cylinders buried in a lossless homogeneous three layer as shown in Figure 1, where (\mathcal{E}_i, σ_i) i=1, 2, 3, denote the permittivities and conductivities in each region. The axis of the buried cylinder is the z axis; that is, the properties of the scatterer may vary with the transverse coordinates only. A group of unrelated incident waves with electric field parallel to the z axis (i.e., transverse magnetic, or TM polarization) is illuminated upon the scatterers.

Owing to the interface, the incident plane wave generates three waves that would exist the absence of the dielectric object. Let the unperturbed field be represented by

$$\vec{E}^{i}(x,y) = \begin{cases}
\left(E_{z}^{i}\right)_{1}(x,y)\hat{z}, & y \geq a, \\
\left(E_{z}^{i}\right)_{2}(x,y)\hat{z}, & a > y > -a, \\
\left(E_{z}^{i}\right)_{3}(x,y)\hat{z}, & y \leq -a.
\end{cases}$$
(1)

Then the internal total electric field inside the dielectric object, $\vec{E}(x,y) = E(x,y)\hat{z} = [E_z^i(x,y) + E_z^s(x,y)]\hat{z}$, can be expressed by the following integral equation:

$$\vec{E}^{i}(\vec{r}) = \int_{s} G(\vec{r}, \vec{r}') k_{2}^{2} \left[\varepsilon_{r}(\vec{r}') - 1\right] E(\vec{r}') ds'$$

$$-j\omega\mu_{0} \int_{c} G(\vec{r}, \vec{r}') J_{s}(\vec{r}') dl' + E(\vec{r}), \quad a > y > -a \quad (2)$$

with

$$G(x, y; x', y') = \begin{cases} G_{1s}(x, y : x', y'), & y \ge a, \\ G_{2s}(x, y; x', y'), & -a < y < a, \\ G_{3s}(x, y; x', y'), & y \le -a, \end{cases}$$
(3a)

Chien-Ching Chiu Author is with the Electrical Engineering Department, Tamkang UniversityTamsui, Taipei, R.O.C. (phone: 886-2621-5656 #2737; fax: 886-2620-9814; e-mail: chiu@ee.tku.edu.tw).

Chun Jen Lin Author is with the Electrical Engineering Department, Tamkang UniversityTamsui, Taipei, R.O.C. (e-mail: lins6619@ms28.hinet.net).

Chung-Hsin Huang is with the Electrical Engineering Department, Tamkang UniversityTamsui, Taipei, R.O.C. (e-mail: 691350010@s91.tku.edu.tw).

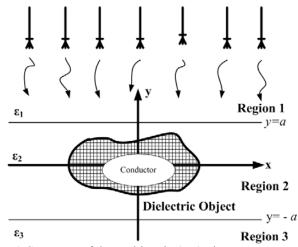


Fig. 1 Geometry of the problem in (x,y) plane

$$G_{ls}(x,y,x',y') = \frac{1}{2\pi} \int_{-\infty}^{\infty} j e^{-j\gamma_1(y-a)} dx$$

$$\frac{(\gamma_2 + \gamma_3) e^{j\gamma_2(y'+a)} + (\gamma_2 - \gamma_3) e^{-j\gamma_2(y'+a)}}{(\gamma_1 + \gamma_2)(\gamma_2 + \gamma_3) e^{j\gamma_2(2a)} + (\gamma_1 - \gamma_2)(\gamma_2 - \gamma_3) e^{-j\gamma_2(2a)}} e^{-j\alpha(x-x')} d\alpha$$

$$G_{2s}(x,y,x',y') = G_{2sf}(x,y,x',y') + G_{2ss}(x,y,x',y')$$
(3b)

 $G_{2s}(x, y, x, y) = G_{2sf}(x, y, x, y) + G_{2ss}(x, y, x, y)$ $G_{3s}(x, y, x', y') = \frac{1}{2\pi} \int_{-\infty}^{\infty} j e^{j\gamma_1(y+a)}$ $(y, +\gamma_2) e^{-j\gamma_2(y'-a)} + (y, -\gamma_1) e^{j\gamma_2(y'-a)}$ (2c)

$$\frac{(\gamma_{1}+\gamma_{2})e^{-j\gamma_{2}(y'-a)}+(\gamma_{2}-\gamma_{1})e^{j\gamma_{2}(y'-a)}}{(\gamma_{1}+\gamma_{2})(\gamma_{2}+\gamma_{3})e^{j\gamma_{2}(2a)}+(\gamma_{1}-\gamma_{2})(\gamma_{2}-\gamma_{3})e^{-j\gamma_{2}(2a)}}e^{-j\alpha(x-x')}d\alpha$$

where

$$G_{2sf}(x, y; x', y') = \frac{j}{4} H_0^{(2)} \left(k_2 \sqrt{(x - x')^2 + (y - y')^2} \right)$$

$$G_{2ss}(x, y, x', y') = \frac{1}{2\pi} \int_{-\infty}^{\infty} \frac{j}{2r_2} \left\{ \frac{\left(r_2 - r_1 \right) \left(r_2 - r_3 \right) \left[e^{-jr_2 \left[\left| y - y' \right| + 2a \right]} + e^{jr_2 \left[\left| y - y' \right| - 2a \right]} \right]}{\left(r_1 + r_2 \right) \left(r_2 + r_3 \right) e^{jr_2 (2a)} + \left(r_1 - r_2 \right) \left(r_2 - r_3 \right) e^{-jr_2 (2a)}} \right]$$

$$+ \frac{\left[\frac{\left(r_2 - r_1 \right) \left(r_2 + r_3 \right) e^{jr_2 \left(\left| y + y' \right|} \right) + \left(r_2 - r_3 \right) \left(r_1 + r_2 \right) e^{-jr_2 \left(\left| y + y' \right|} \right)}{\left(r_1 + r_2 \right) \left(r_2 + r_3 \right) e^{jr_2 (2a)} + \left(r_1 - r_2 \right) \left(r_2 - r_3 \right) e^{-jr_2 (2a)}} \right] e^{-j\alpha(x - x')} d\alpha}$$

$$\gamma_i^2 = k_i^2 - \alpha^2, i = 1, 2, 3, \operatorname{Im}(r_i) \le 0, -a < y' < a$$

Here k_i and \mathcal{E}_r denote the wave number in region i and the relative permittivity of the dielectric objects. J_s is the induced surface current density which i proportional to normal derivative of the electric field on the conductor surface. $H_0^{(2)}$ is the Hankel function of the second kind of order 0. G(x,y;x',y') is the Green's function, which can be obtained by the Fourier transform [10].

The boundary condition states that the total tangential electric field must be zero on the surface of the perfectly conducting cylinder and this yields the following equation:

$$\begin{bmatrix} E^{i}(\vec{r}) = \int_{s} G(\vec{r}, \vec{r}') k_{2}^{2} \left[\varepsilon_{r}(\vec{r}') - 1 \right] E(\vec{r}') ds' \\
- j\omega \mu_{0} \int_{c} G(\vec{r}, \vec{r}') J_{s}(\vec{r}') dl' \right]_{\vec{r} \in c}, \qquad y > -a \qquad (4)$$

The scattered field, $\vec{E}_s(x,y) = E_z^s(x,y)\hat{z}$, can be expressed as

$$E^{s}(\vec{r}) = -\int_{s} G(\vec{r}, \vec{r}') k_{2}^{2} \left[\varepsilon_{r}(\vec{r}') - 1\right] E(\vec{r}') ds'$$
$$+ j\omega \mu_{0} \int_{c} G(\vec{r}, \vec{r}') J_{s}(\vec{r}') dl'$$
 (5)

For the direct scattering problem, the scattered field is computed by giving the permittivity distribution of the buried inhomogeneous dielectric cylinders coated on a conductor objects. This can be achieved by using (2) and (4) to solve the total field inside the object \vec{E} and calculating \vec{E}^s by (5). For numerical implementation of the direct problem, the dielectric objects are divided into N_I sufficient small cells. Similarly, we divide the contour of the conductor into N_2 sufficient small segments so that the induced surface current density can be considered constant over each segment. Thus the permittivity and the total field within each cell can be taken as constants. Then the moment method is used to solve (2), (3) and (4) with a pulse basis function for expansion and point matching for testing. Thus the following matrix equations can be obtained:

$$(E^{i}) = [[G_{1}][\tau] + [I]](E) + [G_{2}](J_{s})$$
(6)

$$(E_{\nu}^{i}) = [G_{3}][\tau](E) + [G_{4}](J_{s})$$
(7)

$$(E^{s}) = -[G_{5}][\tau](E) + [G_{6}](J_{s})$$
(8)

where (E^i) and (E) represent the N_I element incident field column vectors. (E_v^i) is the N_2 element incident field column vectors. (E^s) denotes the M-element scattered field column vectors. Here M is the number of measurement points. The matrices $[G_1]$ and $[G_2]$ are $N_1 \times N_1$ and $N_1 \times N_2$ square matrices, respectively. The matrices $[G_3]$ and $[G_4]$ are $N_2 \times N_1$ and $N_2 \times N_2$ matrices. The matrices $[G_5]$ and $[G_6]$ are $M \times N_1$ and $M \times N_2$ matrices. The element in matrices $[G_i]$, i=1,4,5...,6 can be obtained by tedious mathematic manipulation

 $[\tau]$ is $N_1 \times N_1$ diagonal matrixes whose diagonal element are formed from the permittivities of each cell minus one. [I] is a identity $N_1 \times N_1$ matrix. We can solve the direct problem by using (6)-(8).

We consider the following inverse problem: the permittivity distribution of the inhomogeneous dielectric cylinders coated on a conductor objects buried in a slab medium is to be computed by the knowledge of the scattered field measured in region 1. Note that the only unknown

permittivity is $\mathcal{E}_r(r)$. In the inversion procedure, we choose N_I different incident column vectors. Then (6)-(8) can be expressed as

$$[E_{p}^{i}] = [G_{p1}][\tau] + [I][E]$$
(9)

$$[E_{p}^{s}] = -[G_{p2}][\tau][E]$$
(10)

where

$$[E_{p}^{i}] = [E^{i}] - [G_{2}][G_{4}]^{-1}[E_{v}^{i}]$$

$$[E_{p}^{s}] = [E^{s}] - [G_{6}][G_{4}]^{-1}[E_{v}^{i}]$$

$$[G_{p1}] = [G_1] - [G_2][G_4]^{-1}[G_3]$$

$$[G_{p2}] = [G_6][G_4]^{-1}[G_3] + [G_5]$$

Here $[E_p^i]$ is a $N_1 \times N_1$ matrix. $[E_p^s]$ is a $M \times N_1$ matrix. Note the matrix $[G_6]$ is diagonally dominant and always invertible. It is worth mentioning that other than the matrix $[G_{p2}]$, the matrix $[G_{p1}][\tau]+[I]$ is always well-posed ones in any case. Therefore, by first solving [E] in (9) as well and substituting into (10). Then $[\tau]$ can be found by solving the following equations:

$$[\Psi][\tau] = [\Phi] \tag{11}$$

where

$$[\Phi] = -[E_p^s][E_p^i]^{-1}$$

$$[\Psi] = [E_p^s][E_p^i]^{-1}[G_{p1}] + [G_{p2}]$$

From (11), all the diagonal elements in the matrix $[\tau]$ can be determined by comparing the element with the same subscripts, which may be any row of both $[\Psi]$ and $[\Phi]$:

$$\left(\tau\right)_{nn} = \frac{\left(\Phi\right)_{mn}}{\left(\Psi\right)_{mn}} \tag{12}$$

Note that there are a total of M possible values for each element of τ . Therefore, the average value of these M data is computed and chosen as final reconstruction result in the simulation.

In the above derivation, the key problem is that the incident matrix $[E_p^i]$ must not be a singular matrix, i.e., all the incident column vectors that form the $[E_p^i]$ matrix, must be linearly unrelated. Thus, if the object is illuminated by a group of unrelated incident waves, it is possible to reconstruct the permittivity distribution of the objects. Note that when the number of cells becomes very large; it is difficult to make such a great number of independent measurements. In such a case, some regularization methods must be used to overcome the ill-posedness.

III. NUMERICAL RESULTS

In this section, we report some numerical results obtained by computer simulations using the method described in the Section II. We illustrate the performance of the proposed inversion algorithm and its sensitivity to random noise in the scattered field. Consider a lossless three-layer structure ($\sigma_1 = \sigma_2 = \sigma_3 = 0$) and the width of the second layer is 0.2m. The permittivity in each region is characterized by, $\mathcal{E}_1 = \mathcal{E}_0$, $\mathcal{E}_2 = 2.25\mathcal{E}_0$ and $\mathcal{E}_3 = \mathcal{E}_0$ respectively, as shown in Fig. 1. The frequency of the incident wave is chosen to be 3 GHz and the number of illuminations is the same as that of cells. The incident waves are generated by numerous groups of radiators operated simultaneously.

Each group of radiators is restricted to transmit a narrow-bandwidth pattern that can be implemented by antenna array techniques. By changing the beam direction and tuning the phase of each group of radiators, one can focus all the incident beams in turn at each cell of the object. This procedure is named "beam focusing" [9]. Note that this focusing should be set when the scatterer is absent. Clearly, an incident matrix formed in this way is diagonally dominant and its inverse matrix exists. The measurement is taken from 0.4 m to -0.4 m in region 1 at equal spacing. The number of measurement points is set to be 8 for each illumination. For avoiding trivial inversion of finite dimensional problems, the discretization number for the direct problem is four times that for the inverse problem in our numerical simulation.

The $0.8~\rm cm \times 1.2~\rm cm$ square cross-section of a perfectly conducting rod coated with buried dielectric materials with square cross-sections is discretized into 10×10 cells, and the corresponding dielectric permittivities are plotted in Fig. 2. Each cell has $0.22 \times 0.22~\rm cm$ cross-sections. The reconstructed permittivity distributions of the object are plotted in Fig. 3. The R.M.S. error is about 3.1 % .We can see the reconstruction is also good.

For investigating the effect of noise, we add to each complex scattered field a quantity b+cj, where b and c are independent random numbers having a Gaussian distribution over 0 to the noise level times the R.M.S. value of the scattered field. The noise levels applied include 10^{-5} , 10^{-4} , 10^{-3} , 10^{-2} , and 10^{-1} in the simulations. The numerical results for the example are plotted in Fig. 4. It is seen that the effect of noise is tolerable for noise levels below 1%.

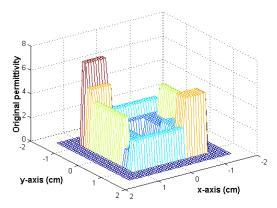


Fig. 2 Original relative permittivity distribution of the dielectric cylinder for the example.

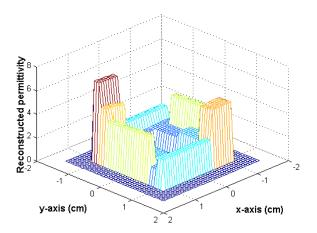


Fig. 3 Reconstructed relative permittivity distribution of the dielectric cylinder for the example.

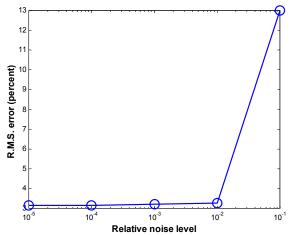


Fig. 3(a) Reconstructed error as a function of the normalized standard deviation of Gaussian noise for the example.

VI. CONCLUSION

In this paper, we propose an efficient algorithm for reconstructing the permittivity distribution of buried inhomogeneous dielectric cylinders coated on a conductor buried in a slab medium has been proposed. By properly arranging the direction and the polarization of various unrelated waves, the difficulty of ill-posedness and nonlinearity is avoided. Thus, the permittivity distribution can be obtained by simple matrix operations. The moment method has been used to transform a set of integral equations into matrix form. Then these matrix equations are solved by the unrelated illumination method. Numerical simulation for imaging the permittivity distribution of a buried inhomogeneous dielectric cylinders coated on a conductor has been carried out and good reconstruction has been obtained even in the presence of Gaussian noise in measured data. This algorithm is very effective and efficient, since no iteration is required.

REFERENCES

[1] A. S. Omar and M. J. Akhtar, "A Generalized Technique for the Reconstruction of Permittivity Profiles With a Controllable Resolution in an Arbitrary Coordinate System" *IEEE Transactions on Antennas and Propagation*, Vol. 53, pp. 294-304, Jan. 2005.

- [2] F. Soldovieri and R. Persico, "Reconstruction of an Embedded Slab from Multifrequency Scattered Field Data under the Distorted Born Approximation", *IEEE Transactions on Antennas and Propagation*, Vol. 52, pp. 2348-2356, Sept. 2004.
- [3] V. A. Mikhnev and P. Vainikainen, "Two-Step Inverse Scattering Method for One-Dimensional Permittivity Profiles", *IEEE Transactions on Antennas and Propagation*, Vol. 48, pp. 293 -298, Feb. 2000.
- [4] K. A. Nabulsi and D. G. Dudley, "A New Approximation and a New Measurable Constraint for Slab Profile Inversion", *IEEE Transactions on Geoscience and Remote Sensing*, Vol. 34, No. 3, May 1996.
- [5] C. C. Chiu and Chun-Jen Lin, "Image Reconstruction of Buried Uniaxial Dielectric Cylinders, " *Electromagnetics*, vol. 22, No. 2, pp. 97-112, Feb. 2002
- [6] Y. S. Lin, C. C Chiu, "Image Reconstruction for a Perfectly Conducting Cylinder Buried in Slab Medium by a TE Wave Illumination", *Electromagnetics*, No. 3, pp. 203-216, April 2005.
- [7] C. J. Lin, C. Y. Chou, and C. C. Chiu, "Electromagnetic Imaging for a Conducting Cylinder Buried in a Slab Medium by the Genetic Algorithm", *International Journal of Imaging Systems and Technology*, Vol. 14, pp. 1-7, June 2004.
- [8] R. F. Harrington, Field Computation by Moment Methods, Macmillan, New York, 1968.
- [9] W. Wang and S. Zhang, "Unrelated Illumination Method for Electromagnetic Inverse Scattering of Inhomogeneous Lossy Dielectric Bodies," *IEEE Transactions on Antennas and Propagation*, vol. AP-40, pp. 1292-1296, Nov. 1992.
- [10] C. C. Chiu and Y. W. Kiang, "Inverse Scattering of a Buried Conducting Cylinder," Inv. Prob., vol. 7, pp. 187-202, April 1991.